Dielectric relaxation measurements on methanol up to the supercritical region

2001 J. Phys.: Condens. Matter 13 10307

(http://iopscience.iop.org/0953-8984/13/46/304)

INSTITUTE OF PHYSICS PUBLISHING JOURNAL OF PHYSICS: CONDENSED MATTER

J. Phys.: Condens. Matter **13** (2001) 10307–10320 PII: S0953-8984(01)25037-1

Dielectric relaxation measurements on methanol up to the supercritical region

Y Hiejima, Y Kajihara, H Kohno and M Yao[1]

Department of Physics, Graduate School of Science, Kyoto University, 606-8502 Kyoto, Japan

E-mail: yao@scphys.kyoto-u.ac.jp (M Yao)

Received 21 May 2001, in final form 31 August 2001
Published 2 November 2001
Online at stacks.iop.org/JPhysCM/13/10307

Abstract

The static permittivity $\varepsilon(0)$ and the dielectric relaxation time τ_D have been obtained for methanol over a wide range of temperature and pressure up to 600 K and 21 MPa. The dielectric relaxation time τ_D decreases with increasing temperature and has little pressure dependence in the liquid state. In the gaseous state, however, τ_D increases with decreasing density. Since these behaviours are qualitatively the same as those for water, we have successfully applied our model for the dielectric relaxation in water to that in methanol with some appropriate modifications.

1. Introduction

Hydrogen-bonded fluids, which attract much interest as supercritical solvents in engineering research fields, are also interesting to study as regards fundamental physics, because their physical properties are strongly state dependent. Recent studies on supercritical alcohols have been prompted by rapid progress in the study of supercritical water. Methanol ($T_c = 512.6$ K, $P_c = 8.10$ MPa and $d_c = 0.272$ g cm^{-3} [1]) has been investigated up to the supercritical region by means of various experimental methods such as PVT [2], nuclear magnetic resonance (NMR) [3–6], Raman scattering [7], x-ray diffraction [8] and neutron diffraction [9] measurements.

The dielectric relaxation, which is a useful probe for the reorientational dynamics of polar molecules, has been investigated for various alcohols where the molecular reorientation is affected by the hydrogen-bond (HB) network. At atmospheric pressure, the dielectric relaxation in liquid methanol has been studied by many authors [10–15] in the temperature range from the melting point [10] to the boiling point [11]. In particular, the dielectric relaxation at room temperature has been measured very precisely by Kaatze *et al* in the frequency range up to 40 GHz [13], by Barthel *et al* up to 295 GHz [14] and by Kindt and Schmuttenmaer up to 1 THz [15]. The measurements reveal that the dielectric relaxation in methanol (also in higher

[1] Author to whom any correspondence should be addressed.

normal alcohols) is represented by a sum of three Debye functions [14–16]. On the other hand, very little is known about the dielectric properties of alcohols at high temperatures and pressures. For methanol, even the static permittivity $\varepsilon(0)$ is available only on the coexistence curve [17] and for the liquid state of density larger than 0.5 g cm^{-3} [18].

Recently we have developed a microwave spectroscopy that can be applied to study the dielectric relaxation of various fluids under high temperatures and pressures in the frequency range up to 40 GHz [19]. By utilizing this technique we have measured the permittivity and the dielectric relaxation time of water and heavy water up to the supercritical state. On the basis of these measurements, we have explained the dielectric relaxation processes of water for the whole fluid phase [20]. In the gaseous state, most water molecules are free from the HB network and they rotate rapidly because of the large thermal energy at high temperatures. The water molecules can respond to the oscillating electric field of the probing microwave only when they lose their rotational energy by mutual collisions. Although most of the water molecules in the liquid state are incorporated in the HB network, they also contribute to the dielectric relaxation when they escape from the network by intermolecular librational motions.

In the present paper, we report the static permittivity $\varepsilon(0)$ and the dielectric relaxation time τ_D for methanol in the temperature and pressure range up to 600 K and 21 MPa. Then we will examine whether our model for the dielectric relaxation processes in water [20] can be applied to those in methanol.

2. Experimental procedure and analysis

Commercially purchased dehydrated methanol (Kanto Chemical Company Incorporated), which has more than 99.8% purity and contains water at less than 0.025%, was used without further purification. The sample was treated in an Ar or He atmosphere to protect it from atmospheric moisture. The sample cell has the shape of a coaxial line (OD 3.0 mm and ID 0.5 mm), and it is composed of platinum outer and inner conductors and quartz glass insulating tubes. In the middle part of the cell is the sample part, where the quartz tube is replaced by the sample. The length of the sample part was 18.6 mm. The sample cell was placed in an internally heated high-pressure vessel pressurized by Ar gas. The dielectric measurements were carried out along either isothermal or nearly isobaric experimental paths in the temperature range up to 600 K and in the pressure range up to 21 MPa. Typical experimental errors in temperature and pressure were less than ± 3 K and ± 0.2 MPa, respectively. A vector network analyser (Wiltron 37269A) was used as both the generator and the receiver of microwaves in the frequency range from 40 MHz to 40 GHz. The network analyser and the device under test (DUT) are connected by coaxial cables whose contributions are removed in advance. The DUT is an assembly of a sample cell and two high-pressure electrodes [19]. The S-matrix which characterizes the DUT was measured directly by the network analyser at each thermodynamic state. The S-matrix consists of four S-parameters, each of which represents either the complex reflection rates (S_{11}, S_{22}) or the complex transmission rates (S_{12}, S_{21}). The uncertainties in the magnitude and the phase of the microwave transmission rate S_{21} or S_{12} were 0.1 dB and 1°, respectively, and those of the reflection rate, S_{11} or S_{22}, were 0.3 dB and 2°, respectively [21]. Note that conventional methods, such as time-domain reflectometry, are not suitable for measurements under extreme conditions, because the calibration procedures are hard to carry out. Further experimental details have been described elsewhere [19, 20].

The static permittivity $\varepsilon(0)$ is calculated with a time-domain analysis, where the impulse response of the DUT is obtained from the Fourier transform of the S-matrix:

$$F_{ij}(t) = \frac{1}{2\pi} \int S_{ij}(\omega) \exp(\mathrm{i}\omega t)\, \mathrm{d}\omega. \tag{1}$$

The time required for the microwave to transmit through the sample part is approximately related to the static permittivity $\varepsilon(0)$ as follows:

$$\frac{l_{\text{sample}}\sqrt{\varepsilon(0)}}{c} = \bar{t}_{21} - \frac{\bar{t}_{11} + \bar{t}_{22}}{2}. \tag{2}$$

Here $\bar{t}_{ij}$ $(i, j = 1, 2)$ is the averaged position of the first peak in $F_{ij}(t)$, defined by

$$\bar{t}_{ij} = \int_{1\text{st peak}} t F_{ij}(t)\,\mathrm{d}t \left(\int_{1\text{st peak}} F_{ij}(t)\,\mathrm{d}t \right)^{-1}. \tag{3}$$

The derivation of (2) is given in appendix A. For water, where the first peak in $F_{ij}(t)$ is sharp, $\bar{t}_{ij}$ in (2) can be simply replaced by the peak position without averaging [19, 20]. However, averaging becomes necessary for methanol, because the peak is very broad and asymmetric, especially at low temperatures.

The S-matrix of the DUT is expressed in terms of the cascade connections of the S-matrices of two high-pressure electrodes, two quartz parts and the sample part [19]. Except for the sample part, the individual S-matrices were measured or calculated in advance. We have to use a model for the sample part to characterize the dielectric relaxation processes of the sample. As the first approximation, we assume that the dielectric relaxation of the sample is described by a Debye function:

$$\varepsilon(\omega) = \varepsilon_\infty + \frac{\varepsilon(0) - \varepsilon_\infty}{1 + \mathrm{i}\omega\tau_{\text{D}}}. \tag{4}$$

Here τ_{D} is the dielectric relaxation time, $\varepsilon(0)$ is the static permittivity obtained from (2) and ε_∞ is the high-frequency permittivity. Other dielectric relaxation functions are also used, when we discuss the relaxation processes in detail in section 4. We assume $\varepsilon_\infty = n^2$, where the refractive index n is obtained from the Lorenz–Lorentz equation

$$\frac{n^2 - 1}{n^2 + 2} = \frac{4\pi\rho\alpha}{3}. \tag{5}$$

Here ρ is the number density and $\alpha = 3.29 \times 10^{-24}$ cm^3 [24] is the polarizability volume. Though we tried fittings for various values of ε_∞ from 1 to 5, the best fitting is achieved when ε_∞ is around n^2. Fixing $\varepsilon(0)$ and ε_∞ in this way, we deduce the dielectric relaxation time τ_{D} that minimizes the residual function

$$R = \sum_i (\log|S_{21}^{\text{cal}}(\omega_i)| - \log|S_{21}^{\text{exp}}(\omega_i)|)^2. \tag{6}$$

Here $S_{21}^{\text{cal}}(\omega_i)$ is the calculated S_{21} at the frequency ω_i, and $S_{21}^{\text{exp}}(\omega_i)$ is the experimental S_{21} at ω_i.

3. Results

3.1. Static permittivity

The static permittivity $\varepsilon(0)$ along the nearly isobaric experimental paths for methanol is shown in figure 1 as a function of temperature at various pressures. The pressures at which the experimental paths cross the saturated vapour pressure curve or the critical isochore are indicated in figure 1. The value of $\varepsilon(0)$ decreases with increasing temperature. At 6.9 MPa, $\varepsilon(0)$ jumps to a smaller value of 1.5 at 510 K and decreases with increasing temperature to 1.3 at 534 K. Above the critical pressure, $\varepsilon(0)$ decreases continuously with increasing temperature. At the critical density, $\varepsilon(0)$ has the value of 2.8 at 520 K and 2.4 at 590 K. Our data at low temperatures are in good agreement with $\varepsilon(0)$ at 0.1 MPa given by Barthel and Neueder [22]

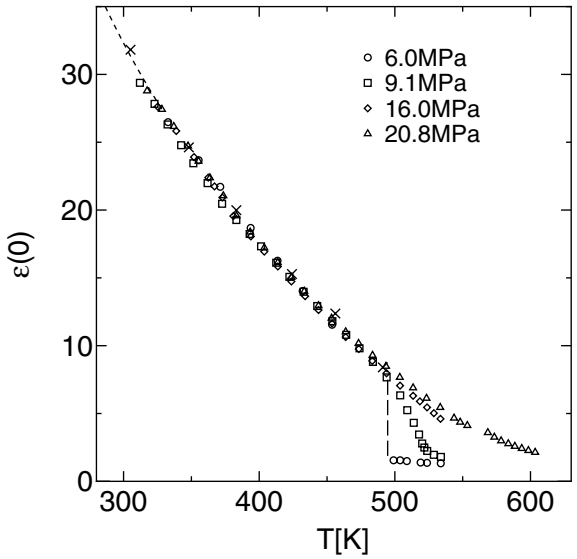

Figure 1. The static permittivity $\varepsilon(0)$ for methanol as a function of temperature. The number attached to each symbol is the pressure at which the nearly isobaric path crosses the coexistence curve or the critical isochore. The broken line and the crosses denote $\varepsilon(0)$ at 0.1 MPa given by Barthel and Neueder [22] and $\varepsilon(0)$ at 10 MPa given by Franck and Deul [18], respectively.

and those at 10 MPa up to 491 K given by Franck and Deul [18] within the experimental error. The error in $\varepsilon(0)$ due to the uncertainty of the sample thickness is estimated to be less than $\pm 4\%$. The numerical values of the static permittivity $\varepsilon(0)$ are given in table 1.

The Kirkwood g-factor g_K [23], which gives a measure of the local ordering of the dipoles, is defined by

$$\frac{(\varepsilon(0)-1)(2\varepsilon(0)+1)}{9\varepsilon(0)} = \frac{4\pi\mu^2\rho}{9k_BT}g_K \tag{7}$$

where ρ is the number density and $\mu = 1.7$ D [24] is the dipole moment of a methanol molecule. The value of g_K is 4.9 at room temperature and decreases with decreasing density. At the critical density, g_K has a value around 1.4, approaching unity at the dilute limit. The behaviour of g_K may suggest that the dipole moment of the methanol molecule prefers parallel orientations due to the hydrogen bonding in the liquid state, and the orientational correlation becomes weak with decreasing density.

3.2. Dielectric relaxation time

The dielectric relaxation time τ_D is shown in figure 2 as a function of temperature at various pressures. The values given in figure 2 are again the pressures at which the experimental paths cross the saturated vapour pressure curve or the critical isochore. The present τ_D at low temperatures are in good agreement with those reported by Jordan *et al* [11] at 0.1 MPa up to 313 K. The latter is shown by the crosses in figure 2. In the liquid state, τ_D decreases rapidly with increasing temperature irrespectively of pressure. At 7.9 MPa, τ_D jumps to a larger value at the boiling temperature. In the gaseous state, τ_D increases with increasing temperature and strongly depends on pressure.

The density dependence of τ_D is shown in figure 3 by the open symbols. Here the density is calculated from the equation of state given by Goodwin [25]. At low temperatures, τ_D is

Table 1. The numerical values of the static permittivity $\varepsilon(0)$ and the dielectric relaxation time τ_D for methanol.

T (K)	P (MPa)	d (g cm^{-3})	$\varepsilon(0)$	τ_D (ps)
322	8.3	0.78	27.8	30.4
372	8.8	0.73	20.5	14.5
372	14.5	0.74	20.9	14.4
373	18.7	0.74	21.1	14.4
423	7.5	0.67	15.7	7.1
423	14.9	0.68	14.7	6.9
423	19.4	0.69	15.0	7.1
473	8.9	0.59	9.8	4.0
473	15.3	0.61	9.8	4.1
493	9.0	0.53	7.7	3.5
493	15.5	0.57	8.0	3.6
493	20.2	0.59	8.5	3.7
513	9.0	0.42	4.3	3.5
513	15.6	0.52	6.3	3.2
513	20.5	0.55	6.9	3.2
533	10.0	0.17	2.0	6.5
533	10.8	0.25	2.6	4.5
533	11.6	0.33	3.1	3.6
533	12.1	0.36	3.6	3.3
533	12.8	0.39	4.0	3.2
533	13.7	0.42	4.2	3.2
533	14.8	0.44	4.4	3.2
533	15.6	0.45	4.6	3.1
533	20.6	0.50	5.4	3.0
543	20.7	0.47	4.7	3.0
553	20.7	0.44	4.1	3.0
593	20.8	0.28	2.4	3.8

weakly dependent on density and is strongly dependent on temperature. In the supercritical states, however, τ_D has little temperature dependence and increases with decreasing density. The numerical values of the dielectric relaxation time τ_D are given in table 1. The major source of the experimental error in τ_D is in the selection of ε_∞, and the error in τ_D is estimated to be less than ± 1 ps.

4. Discussion

At low temperatures, the most relevant parameter determining the dielectric relaxation time is the temperature. Above the critical temperature, however, the temperature dependence of τ_D becomes very small, and τ_D increases remarkably with decreasing density. Since these behaviours are qualitatively the same as those in water, our model for the dielectric relaxation

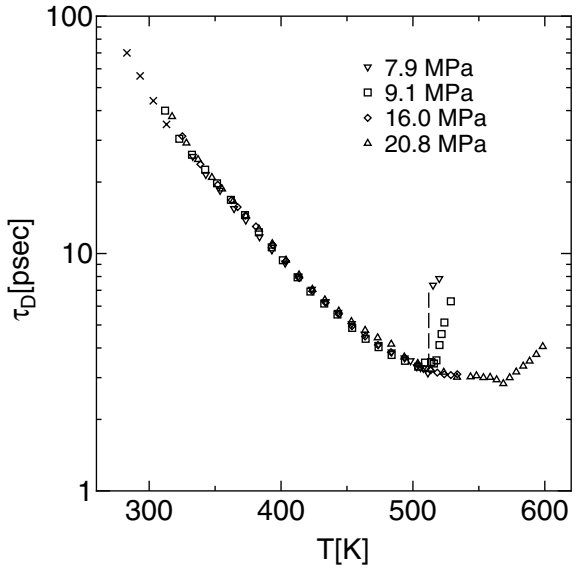

Figure 2. The dielectric relaxation time τ_D for methanol as a function of temperature. The number attached to each symbol is the pressure at which the nearly isobaric path crosses the coexistence curve or the critical isochore. The crosses denote τ_D at 0.1 MPa given by Jordan *et al* [11].

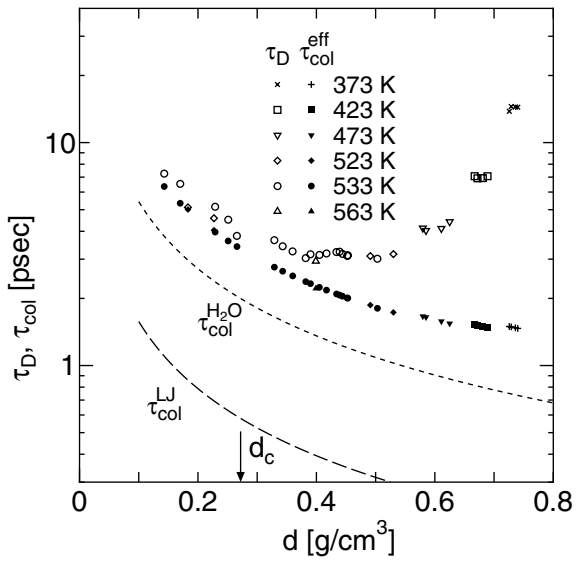

Figure 3. The dielectric relaxation time τ_D (open symbols) and the effective binary collision time τ_{col}^{eff} (closed symbols) for methanol at various temperatures are plotted as a function of density. Here τ_{col}^{eff} is calculated from (8) for $\sigma_{eff} = 7$ Å^2. The broken line and the dotted line are the binary collision times at 533 K for $\sigma^{LJ} = 40$ Å^2 and $\sigma^{H_2O} = 11.7$ Å^2, respectively. The critical density d_c is shown by the arrow.

in water [20] is expected to be applicable to methanol. In what follows, we give a brief review on the dielectric relaxation of water first, and we proceed to interpret the dielectric relaxation of methanol.

4.1. Dielectric relaxation in water

In the gaseous state, the dielectric relaxation time τ_D of water has been well described with the binary collision time τ_{col} [20] defined by [26]

$$\tau_{col} = \frac{1}{4\rho\sigma}\sqrt{\frac{m\pi}{k_B T}}. \tag{8}$$

Here m is the mass of a water molecule, ρ is the number density and $\sigma = 11.6$ Å^2 is the cross section of a water molecule, which is estimated from the intramolecular O–H distance. The water molecules are free from the HB network and rotate rapidly, and they are insensitive to the change of the applied electric field unless they collide with each other and lose their rotational energy.

In the high-temperature liquid state, τ_D for water deviates from τ_{col}, which should be associated with the hydrogen bonding. In addition to the free water molecules, those molecules which are bound to the HB network may contribute to the dielectric relaxation. Thus, the complex permittivity $\varepsilon(\omega)$ may be written as [20]

$$\varepsilon(\omega) = \varepsilon_\infty + (1 - f_B)\frac{\varepsilon(0) - \varepsilon_\infty}{1 + i\omega\tau_{fast}} + f_B\frac{\varepsilon(0) - \varepsilon_\infty}{1 + i\omega\tau_{slow}} \tag{9}$$

where f_B is the fraction of the bound molecules. The second term represents the contribution of the free molecules and the third term represents that of the bound molecules, and τ_{fast} and τ_{slow} are the corresponding relaxation times. We have assumed

$$\tau_{fast} = \tau_{col} \tag{10}$$

for the whole fluid phase, though τ_{fast} may be modified in the liquid state. It is interesting that τ_{col} from (8) has a value of 0.3 ps at room temperature, which is close to the second relaxation time of 0.2 ps at 303 K obtained from the dielectric relaxation measurements up to higher frequencies [27].

The relaxation time of the bound molecules τ_{slow} may be described as a sum of τ_{col} and the escape time τ_B, the latter of which is the time taken for water molecules to escape from the HB network:

$$\tau_{slow} = \tau_{col} + \tau_B. \tag{11}$$

On the assumption that the breaking of the hydrogen bond is promoted by the librational motions of water molecules, the escape time τ_B is written as

$$\tau_B = \langle\tau_{lib}\rangle \exp[\Delta H/k_B T] \tag{12}$$

where $\langle\tau_{lib}\rangle = 0.067$ ps is the inverse of the mean librational frequency of the hydrogen-bonded water molecule and $\Delta H = 10.6$ kJ mol^{-1} is the enthalpy of hydrogen bonding, both of which have been determined from Raman scattering measurements [28]. To estimate the contribution of the bound molecules, we have equated the observed dielectric relaxation time τ_D with the average relaxation time τ_{ave} defined as

$$\tau_{ave} = (1 - f_B)\tau_{fast} + f_B\tau_{slow}. \tag{13}$$

The fraction of bound molecules f_B is found to be consistent with the number of hydrogen bonds per molecule divided by four, $N_{HB}/4$, estimated from neutron diffraction measurements [29] and NMR measurements [30].

In the temperature range below 350 K, the dielectric relaxation time becomes much longer, which would make f_B larger than unity. This discrepancy may be reconciled by introducing an enhancement of the escape time. The enhancement factor η may be described as

$$\tau_D = \tau_{col} + \eta\tau_B. \tag{14}$$

This treatment corresponds to the case where $f_B = 1$ in (9) and τ_B in (11) are replaced by $\eta\tau_B$. Here η could be physically interpreted, for instance, as the rate at which a water molecule, once separated from the HB network, is recaptured by the HB network, and τ_D may be the mean time of the distribution of the relaxation time. It has been found from experiment that the enhancement factor η has the functional form

$$\frac{1}{\eta} = \frac{T - T_0}{T_x - T_0} \tag{15}$$

where $T_x = 352$ K may be regarded as the crossover temperature [20, 31] and $T_0 = 221$ K as the stability-limit temperature [32].

4.2. Dielectric relaxation in methanol

The density dependence of the dielectric relaxation time τ_D at constant temperatures is shown for methanol by the open symbols in figure 3. The negative density dependence of the dielectric relaxation time τ_D at low densities suggests that the dielectric relaxation of gaseous methanol can also be described as binary collisions. The binary collision time τ_{col} is defined by (8), where m and σ should be replaced by the values for methanol. If we were to estimate the cross section σ from the Lennard-Jones diameter [26], that is $\sigma_{LJ} = 40$ Å^2, the binary collision time τ_{col}^{LJ}, denoted by the broken line at 533 K in figure 3, would have a value much smaller than τ_D, though their slopes are much alike. This implies that the effective cross section may be smaller than the value estimated from the molecular size. If we take the same cross section as that for water, $\sigma_{H_2O} = 11.7$ Å^2, the estimated collision time $\tau_{col}^{H_2O}$, denoted by the dotted line at 533 K in figure 3, also underestimates the experimental τ_D. Then we determine the effective cross section σ_{eff} in such a way that the corresponding collision time reproduces the observed density dependence of τ_D at low densities. This gives 6–9 Å^2 for σ_{eff}. The effective binary collision time τ_{col}^{eff} for $\sigma_{eff} = 7$ Å^2 is plotted as closed symbols for various temperatures in figure 3. The value of σ_{eff} is appreciably smaller than σ_{H_2O}. This may be explained as follows. The effective cross section for a methanol molecule may be determined by the OH group which should play an important role in the dielectric relaxation. The cross section of the OH group is expected to be close to that of water, but it may be reduced due to the steric hindrance by the hydrophobic CH_3 group. It is interesting to note that τ_{col}^{eff} for methanol at room temperature (=1.5 ps) is close to the second relaxation time $\tau_2 = 1.25$ ps at room temperature [15]. The corresponding values of τ_{col}^{LJ} (=0.1 ps) and $\tau_{col}^{H_2O}$ (=0.7 ps) are much smaller than τ_{col}^{eff} and τ_2.

While the dielectric relaxation time τ_D strongly depends on density in the gaseous state, the density dependence of τ_D at constant temperatures becomes much weaker in the liquid state, where the relevant parameter is the temperature. Thus, it is suggested that the contribution of the molecules which are incorporated in the HB network should be important in the liquid state. Although most methanol molecules are incorporated in the twofold-coordinated HB network in the liquid state, these methanol molecules are also expected to participate in the dielectric relaxation when they have a chance to escape from the network. In contrast to the case for water, where the librational motions play the most important role in the breaking of the hydrogen bonds, the hydrogen bonds in methanol may be broken by the intermolecular stretching motion. Since methanol has a chain-like structure, the hydrogen-bond breaking is likely to occur when it is elongated. The importance of the stretching modes is suggested by the fact that they have the highest energy among the intermolecular modes [33–35], which is also true for the librational modes of water [28]. In other words, both the stretching modes of methanol and the librational modes of water are the most frequent intermolecular vibrations.

Then, instead of (12), the escape time τ_B for methanol may be described as

$$\tau_B = \langle \tau_{stretch} \rangle \exp[\Delta H / k_B T]. \tag{16}$$

Here $\langle \tau_{stretch} \rangle$ is the characteristic time of the stretching motion of the hydrogen-bonded molecule and ΔH is the enthalpy of hydrogen bonding. ΔH is given as 11.3 kJ mol^{-1} by the Raman scattering study for liquid methanol [36], and $\langle \tau_{stretch} \rangle$ is given as 0.280 ps by the infrared absorption study [33].

Although τ_D is useful for characterizing the dielectric relaxation processes of methanol over the whole fluid phase, it is more consistent to use a sum of two Debye functions as the relaxation function, when both the free and bound molecules contribute to the relaxation processes. Thus, we analyse our data with a model whose relaxation function is a sum of two Debye functions given by (9). Here the relaxation times τ_{fast} given by (10) and τ_{slow} given by equations (11) and (16) are fixed during the fitting procedure: only f_B is treated as a fitting parameter. The resultant f_B at constant temperatures are plotted as a function of density in figure 4. For comparison, the degree of hydrogen bonding obtained from NMR measurements [4] and the number of hydrogen bonds per molecule divided by two, $N_{HB}/2$, obtained from neutron diffraction study [9] are also plotted. Our f_B is consistent with the corresponding quantities, though the error bars estimated from the uncertainty of determining σ are relatively large at low densities.

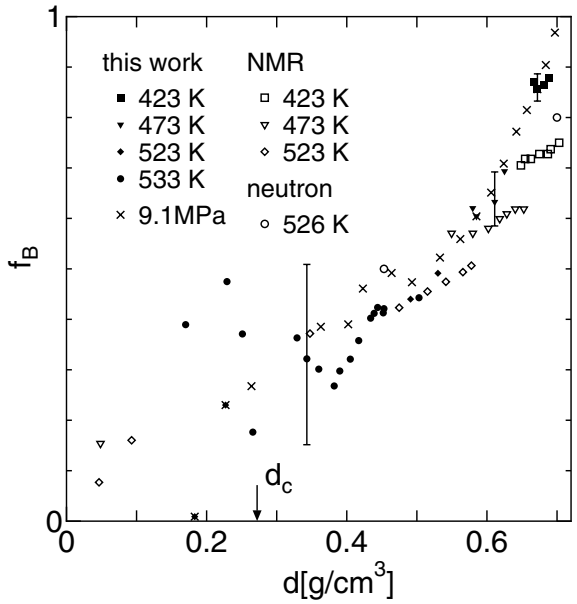

Figure 4. The fraction of bound molecules f_B for $\sigma_{eff} = 7$ Å^2 is plotted against density. The closed symbols correspond to f_B at the given temperatures and the crosses correspond to those along the nearly isobaric path at 9.1 MPa. The error bars are estimated from the uncertainty in determining σ. The degrees of hydrogen bonding obtained from NMR measurements by Hoffmann and Conradi [4] at various temperatures are shown by the open symbols. The open circles each denote half of the number of hydrogen bonds per molecule, obtained from neutron diffraction measurements by Yamaguchi *et al* [9]. The critical density d_c is also shown by the arrow.

In figure 5, τ_{ave} defined by (13) and τ_D along the nearly isobaric path at 9.1 MPa are plotted as a function of temperature. The corresponding f_B has already been shown in figure 4 by the crosses. At high temperatures, the agreement between τ_{ave} and τ_D is fairly good. Thus, τ_D can

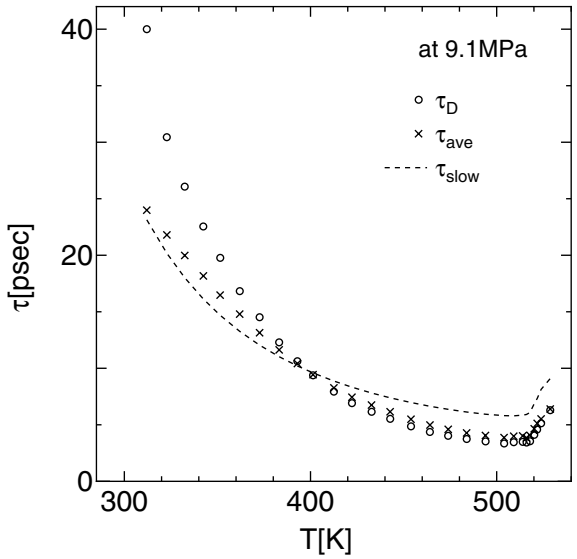

Figure 5. The dielectric relaxation time τ_D (○) and the average relaxation time τ_{ave} (×) are shown as a function of temperature. The corresponding slower relaxation time τ_{slow} is also plotted as the broken line. These values are obtained from the data along the nearly isobaric experimental path at 9.1 MPa.

be interpreted as the average of two relaxation times. At low temperatures below 400 K, τ_{ave} exceeds the slower relaxation time τ_{slow}. This indicates that our two-Debye-function model is not effective at low temperatures. Moreover, the residual function R defined by (6) for our two-Debye-function model has a much larger value than that for our one-Debye-function model. The molecular motions are expected to be strongly correlated at low temperatures and high densities, and the correlation leads to a distribution of relaxation times. Then, we analysed the data with a Cole–Cole function. However, the exponent $1-\alpha$ is found to range from 0.98 to 1, which means that the relaxation process is practically described by one Debye function. Thus, we interpret τ_D in the same manner as for water at low temperatures—that is, the strong correlation is characterized by the enhancement of τ_B. In fact, τ_D deviates upwards from τ_{slow} at low temperatures.

The reciprocal of the enhancement factor η (see (14)) is plotted against temperature in figure 6. The error bars are estimated from the temperature dependence of $\langle\tau_{stretch}\rangle$ [33] and the uncertainty in ΔH [36]. It is found that $1/\eta$ decreases gradually with decreasing temperature, which is clearly different from the case for water described by (15), where the enhancement seems to diverge near the stability-limit temperature. The double-logarithm plot is shown in figure 6(b). The slope of $1/\eta$ shows an obvious change around 400 K, where $\eta \simeq 1$. At lower temperatures, the symbols lie on a line whose slope is 2.0. Thus, $1/\eta$ at temperatures below 400 K can be empirically described as

$$1/\eta \approx (T/T_x)^{\beta} \tag{17}$$

with $\beta \approx 2.0$ and $T_x \approx 407$ K. At finite temperature, η does not diverge, which implies absence of the stability limit. It is plausible that the motion of methanol molecules is not so strongly correlated as that of water molecules, because the methanol molecules have only two hydrogen bonds per molecule and hence they are less constrained than the water molecules which are incorporated in the tetrahedrally coordinated HB network.

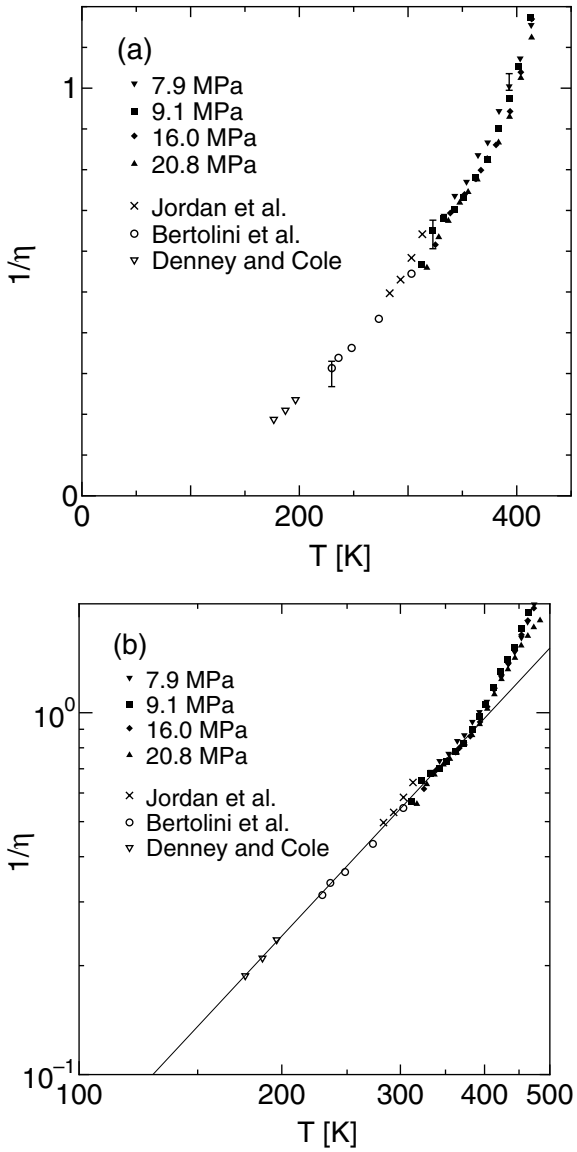

Figure 6. The inverse of the enhancement factor, $1/\eta$, is plotted against T. The values obtained from Jordan *et al* [11], Bertolini *et al* [12] and Denney and Cole [10] are also plotted. The thin line in (b) denotes the relation given by (17) with $T_x = 407$ K and $\beta = 2.0$.

5. Summary and outlook

We have measured the static permittivity $\varepsilon(0)$ and the dielectric relaxation time τ_D for fluid methanol up to 600 K and 21 MPa with microwave spectroscopy. In the liquid state, $\varepsilon(0)$ and τ_D decrease with increasing temperature. At the liquid–gas transition, $\varepsilon(0)$ jumps to a smaller value, and τ_D jumps to a larger value. The most relevant parameter determining τ_D is the temperature at high densities or at low temperatures, and it is the density at low densities or at high temperatures which is qualitatively the same as that of water.

We have modified our model for the dielectric relaxation of water to explain the dielectric relaxation in methanol over the whole fluid phase. In the gaseous state, τ_D increases with decreasing density with weak temperature dependence. These behaviours have been explained on the basis of binary collisions, whose cross section has been found to be appreciably smaller than that expected from the molecular dimensions. The degree of hydrogen bonding has been estimated on the assumption that the breaking of the hydrogen bond is promoted by the stretching mode rather than the librational modes in water. Though the increase of τ_D in liquid methanol has been observed in the low-temperature region, the enhancement of τ_D has weaker temperature dependence than that for liquid water, which may be a consequence of methanol being less constrained than water.

Acknowledgments

The authors are grateful to Professor T Yamaguchi for valuable discussions, to Dr K Okada for helpful advice, to Mr N Itokawa and Mr K Furuta for collaboration on the experiments.

Appendix A.

The normalized response function $\tilde{F}_{ij}(t)$ is related to $S_{ij}(\omega)$ by

$$\frac{S_{ij}(\omega)}{S_{ij}(0)} = \int \tilde{F}_{ij}(t)\mathrm{e}^{-\mathrm{i}\omega t}\,\mathrm{d}t. \tag{A.1}$$

Here $\tilde{F}_{ij}(t)$ is defined as

$$\tilde{F}_{ij}(t) = F_{ij}(t)\left(\int_{1\text{st peak}} F_{ij}(t)\,\mathrm{d}t\right)^{-1}. \tag{A.2}$$

Differentiating (A.1) with respect to ω and putting $\omega = 0$, we obtain

$$\frac{S'_{ij}(0)}{S_{ij}(0)} = (-\mathrm{i})\int t\tilde{F}_{ij}(t)\,\mathrm{d}t = (-\mathrm{i})\bar{t}_{ij} \tag{A.3}$$

where $\bar{t}_{ij}$ is the mean time in $\tilde{F}_{ij}(t)$. Using (A.3), the average transit time

$$\Delta\bar{t} \equiv \bar{t}_{21} - (\bar{t}_{11} + \bar{t}_{22})/2$$

is written as

$$\Delta\bar{t} = \mathrm{i}\,\frac{\mathrm{d}}{\mathrm{d}\omega}\left[\ln S_{21}(\omega) - \frac{1}{2}(\ln S_{11}(\omega) + \ln S_{22}(\omega))\right]\Bigg|_{\omega=0}. \tag{A.4}$$

Now we consider a cascade connection of a quartz part (of length l_1), the sample part (of length l) and another quartz part (of length l_2). The elements of the S-matrix corresponding to the first peak in $F_{ij}(t)$, where the multiple reflections are ruled out, are described as

$$S_{11}(\omega) = \frac{z(\omega) - z_Q}{z(\omega) + z_Q}\exp[-2\gamma_Q l_1] \tag{A.5}$$

$$S_{22}(\omega) = \frac{z(\omega) - z_Q}{z(\omega) + z_Q}\exp[-2\gamma_Q l_2] \tag{A.6}$$

$$S_{21}(\omega) = \frac{4z_Q z(\omega)}{(z(\omega) + z_Q)^2}\exp[-\gamma_Q l_1 - \gamma_Q l_2 - \gamma(\omega)l]. \tag{A.7}$$

Here $z(\omega)$ is the characteristic impedance and $\gamma(\omega)$ is the propagation factor. z_Q and γ_Q are the corresponding values for the quartz parts. $z(\omega)$ and $\gamma(\omega)$ are described as

$$z(\omega) = \frac{1}{2\pi}\sqrt{\frac{\mu_0}{\epsilon_0 \varepsilon(\omega)}}\ln(R_{out}/R_{in}) \tag{A.8}$$

$$\gamma(\omega) = \frac{i\omega\sqrt{\varepsilon(\omega)}}{c} \tag{A.9}$$

where ϵ_0 and μ_0 are the permittivity and the permeability in vacuum, and R_{out} and R_{in} are the outer and inner radius of the coaxial line. Then, by combining (A.4) with (A.5)–(A.9), $\Delta\bar{t}$ is expressed as

$$\Delta\bar{t} = \frac{l\sqrt{\varepsilon(0)}}{c} - \frac{i}{2\varepsilon(0)}\frac{\varepsilon(0)+\varepsilon_Q}{\varepsilon(0)-\varepsilon_Q}\left.\frac{d\varepsilon(\omega)}{d\omega}\right|_{\omega=0}. \tag{A.10}$$

Practically, we have used only the first term of the right-hand side of (A.10), because the second term is estimated to be much smaller than the first one. In fact, when we assume that $\varepsilon(\omega)$ has the form of a Debye function:

$$\left.\frac{d\varepsilon(\omega)}{d\omega}\right|_{\omega=0} = -i(\varepsilon(0)-\varepsilon_\infty)\tau \tag{A.11}$$

the second term on the right-hand side of (A.10) is smaller than the first term by more than one order of magnitude, except for the region where $\varepsilon(0) \simeq \varepsilon_Q$.

References

[1] Kay W B and Donham W E 1955 *Chem. Eng. Sci.* **4** 1
[2] Straty G C, Palavra A M F and Bruno T J 1986 *Int. J. Thermophys.* **7** 1077
[3] Asahi N and Nakamura Y 1998 *J. Chem. Phys.* **109** 9879
[4] Hoffmann M M and Conradi M S 1998 *J. Phys. Chem.* B **102** 263
[5] Bai S and Yonker C R 1998 *J. Phys. Chem.* A **102** 8641
[6] Müßig S, Franck E U and Holz M 2000 *Z. Phys. Chem.* **214** 957
[7] Ebukuro T, Takami A, Ohshima Y and Koda S 1999 *J. Supercrit. Fluids* **15** 73
[8] Yamaguchi T 1998 *J. Mol. Liq.* **78** 43
[9] Yamaguchi T, Bennmore C J and Soper A K 2000 *J. Chem. Phys.* **112** 8976
[10] Denney D J and Cole R H 1955 *J. Chem. Phys.* **23** 1767
[11] Jordan B P, Sheppard R J and Szwarnowski S 1978 *J. Phys. D: Appl. Phys.* **11** 695
[12] Bertolini D, Cassettari M and Salvetti G 1983 *J. Chem. Phys.* **78** 365
[13] Kaatze U, Schäfer M and Pottel R 1989 *Z. Phys. Chem. NF* **165** 103
[14] Barthel J, Bachhuber K, Buchner R and Hetzenauer H 1990 *Chem. Phys. Lett.* **165** 369
[15] Kindt J T and Schmuttenmaer C A 1996 *J. Phys. Chem.* **100** 10 373
[16] Garg S K and Smyth C P 1965 *J. Phys. Chem.* **69** 1294
[17] Dannhauser W and Bahe J W 1964 *J. Chem. Phys.* **40** 3058
[18] Franck E U and Deul R 1978 *Faraday Discuss. Chem. Soc.* **66** 191
[19] Okada K, Imashuku Y and Yao M 1997 *J. Chem. Phys.* **107** 9302
[20] Okada K, Yao M, Hiejima Y, Kohno H and Kajihara Y 1999 *J. Chem. Phys.* **110** 3026
[21] *Technical Data Sheet, Wiltron 37200A Series Microwave Vector Network Analyzer* 1994 Wiltron Company, Morgan Hill, CA
[22] Barthel J and Neueder N 1992 *Electrolyte Data Collection* Part 1, vol 12 (Frankfurt: Dechema)
[23] Hansen J-P and McDonald I R 1986 *Theory of Simple Liquids* 2nd edn (London: Academic)
[24] *CRC Handbook of Chemistry and Physics* 1987 68th edn (Boca Raton, FL: Chemical Rubber Company Press)
[25] Goodwin R D 1987 *J. Phys. Chem. Ref. Data* **16** 799
[26] Hirschfelder J O, Curtis C F and Bird R B 1954 *Molecular Theory of Gases and Liquids* (New York: Wiley)
[27] Rønne C, Thrane L, Åstrand P-O, Wallqvist A, Mikkelsen K V and Keidung S R 1997 *J. Chem. Phys.* **107** 531
[28] Carey D M and Korenowski G M 1998 *J. Chem. Phys.* **108** 2669
[29] Jedlovszky P, Brodholt J P, Bruni F, Ricci M A, Soper A K and Vallauri R 1998 *J. Chem. Phys.* **108** 8528

[30] Matubayasi N, Wakai C and Nakahara M 1997 *J. Chem. Phys.* **107** 9133
[31] Yoshii N, Yoshie H, Miura S and Okazaki S 1998 *J. Chem. Phys.* **109** 4873
[32] Speedy R J and Angell C A 1976 *J. Chem. Phys.* **65** 851
[33] Passchier W F, Klompmaker E R and Mandel M 1970 *Chem. Phys. Lett.* **4** 485
[34] Vij J K, Reid C J and Evans M W 1983 *Mol. Phys.* **50** 935
[35] Lake R F and Thompson H W 1966 *Proc. R. Soc.* A **291** 469
[36] Edwards H G M and Farwell D W 1990 *J. Mol. Struct.* **220** 217